NREL/TP-442-5225 • UC Category: 261 • DE93000041

Full Vector (3-D) Inflow Simulation in Natural and Wind Farm Environments Using an Expanded Version of the SNLWIND (VEERS) Turbulence Code

N. D. Kelley

Prepared for 12th ASME Wind Energy Symposium
Houston, Texas
31 January – 4 February, 1993

National Renewable Energy Laboratory
1617 Cole Boulevard
Golden, Colorado 80401-3393
A Division of Midwest Research Institute
Operated for the U.S. Department of Energy
under Contract No. DE-AC02-83CH10093

Prepared under Task No. WE218001

November 1992

On September 16, 1991 the Solar Energy Institute was designated a national laboratory, and its name was changed to the National Renewable Energy Laboratory.

Printed in the United States of America
Available from:
National Technical Information Service
U.S. Department of Commerce
5285 Port Royal Road
Springfield, VA 22161

Price: Microfiche A01
Printed Copy A02

Codes are used for pricing all publications. The code is determined by the number of pages in the publication. Information pertaining to the pricing codes can be found in the current issue of the following publications which are generally available in most libraries: *Energy Research Abstracts (ERA)*; *Government Reports Announcements* and Index (*GRA* and I); *Scientific and Technical Abstract Reports (STAR)*; and publication NTIS-PR-360 available from NTIS at the above address.

FULL VECTOR (3-D) INFLOW SIMULATION IN NATURAL AND WIND FARM ENVIRONMENTS USING AN EXPANDED VERSION OF THE SNLWIND (VEERS) TURBULENCE CODE

N.D. Kelley
National Renewable Energy Laboratory
Golden, Colorado

ABSTRACT

We have recently expanded the numerical turbulence simulation (SNLWIND) developed by Veers [1] to include all three components of the turbulent wind vector. We have also configured the code to simulate the characteristics of turbulent wind fields upwind and downwind of a large wind farm, as well as over uniform, flat terrain. Veers's original method only simulates the longitudinal component of the wind in neutral flow. This paper *overviews* the development of spectral distribution, spatial coherence, and cross-axis correlation models used to expand the SNLWIND code to include the three components of the turbulent wind over a range of atmospheric stabilities. These models are based on extensive measurements of the turbulence characteristics immediately upwind and downwind of a large wind farm in San Gorgonio Pass, California.

NOMENCLATURE

b_i = coherence decrement of i-th wind component
c_p = specific heat at constant pressure
f = reduced frequency, $f = nz/U$
f_i = reduced frequency, $f_i = nz_i/U$
f_m = reduced frequency value at peak of $nS(n) / u_*^2$
g = gravity acceleration
H = vertical heat flux
L = Obukhov length, $-u_*^3 c_p \rho T / gH\kappa$
n = cyclic frequency (Hz)
p = atmospheric pressure
$r_{i,j}$ = normalized cross-axis correlation function
Ri = gradient Richardson number, $(g/\Theta)[(\partial\theta/\partial z)/(\partial U/\partial z)^2]$
$S_\xi(n)$ = spectral density of ξ
T = sensible absolute air temperature
u_{*_o} = friction velocity derived from velocity profile
u_* = measured local friction velocity at hub height
u = longitudinal velocity component
U_H = mean horizontal wind speed
U_{hub} = mean horizontal wind speed at hub height
v = crosswind or lateral velocity component
w = vertical wind component
z = height above local terrain
z_{hub} = average wind farm hub height
z_{ref} = reference height within turbine rotor disk
z_i = height of first temperature inversion
z_o = surface roughness length
z/L = expression of surface layer stability
κ = von Karman constant (≈ 0.4)
θ = potential temperature, $T(1000/p)^{.286}$
Θ = layer mean potential temperature
ρ = air density
Φ_i = local/smooth terrain spectral peak position ratio
Ψ_i = local/smooth terrain spectral peak ratio
$(')$ = denotes fluctuating quantity with zero mean

INTRODUCTION

A crucial issue in the ability of numerical simulations to model the dynamic response of wind turbines is the credibility of the input flow field used to excite the turbine and its components. Veers [2] has developed a simulation (known as SNLWIND or the "Sandia Method") that generates a full spatial distribution of the time-varying, longitudinal or streamwise (u) wind component. He later simplified the process for horizontal-axis wind turbines (HAWTs) by modeling the wind at a finite number of points at the moment of blade passage [1].

Kelley and Wright [3] have recently compared the Veers HAWT model predictions with observed data derived from measurements up- and downwind of a large wind farm in San

Gorgonio Pass, California. They found that SNLWIND does a good job of simulating many of the properties of the flow upwind of the wind farm under unstable and near-neutral stability conditions. Because it only simulates the *u*-component, it cannot account for the substantial turbulent energy observed in the crosswind (*v*) and vertical (*w*) components. As would be expected, it also underpredicts the high levels of small-scale turbulence experienced downwind (and within) the wind farm. This discrepancy becomes smaller as the mean wind speed and stability increase. Again, the substantial turbulent energy, particularly in the crosswind (*v*) component, is unaccounted for.

Recent measurements [4] have indicated that the temporal and spatial coherence of the inflow turbulence may be associated with many of the observed extreme structural load events. Several such extreme structural and peak power episodes have been traced to periods when the turbine rotor encountered patches of coherent turbulence. These coherent structures are identified by short-lived excursions in the turbulent vorticity and shear stress components. The use of only the longitudinal or *axial* (*u*) wind component in turbine dynamics modeling may preclude the identification of important structural responses that are sensitive to turbulent fluctuations in the *inplane* or crosswind (*v*) and vertical (*w*) components.

To provide a more realistic turbulent inflow for the dynamic modeling of wind turbine structures, the author has expanded the original Veers simulation to include all three components of the wind vector: *u*, *v*, and *w*. Because of space limitations, only an *overview* the expansion is presented. The development of models for the velocity variance spectra, spatial coherence, and cross-axis component correlations are discussed. These models reflect the statistical characteristics of the turbulent inflows up- and downwind of a 41-row wind farm located in the San Gorgonio Pass of Southern California. The goal of this work is to use the "Sandia Method" to numerically generate a *statistically relevant* ten-minute record or realization of the three-dimensional turbulent wind. This record emulates the temporal and spatial variations of the three-dimensional wind vector that can be expected in the real wind in and near a large wind farm.

Veers incorporates a Fourier synthesis method in which "target" analytical models for the longitudinal (*u*) velocity spectrum and spatial coherence are used as the basis for the frequency-to-time domain transformation. Veers recommends the spectral and coherence models developed by Solari [5] which assume neutrally-stable flow over flat, uniform, or aerodynamically smooth terrain.

The author extended the single-velocity component form of the SNLWIND code to the three components by first identifying suitable smooth-terrain spectral models to use as a reference. He then used an extensive set of measurements from two towers installed up- and downwind of the wind farm to develop empirical functions relating available boundary-layer scaling parameters and the following:

- Velocity component spectra, $S_\xi(n)$
- Vertical coherence of the streamwise (b_u) and crosswind (b_v) wind components
- Normalized cross-axis component correlations (r_{ij})

VELOCITY SPECTRAL MODEL DEVELOPMENT

The author's approach has been to identify suitable spectral models that provide a good statistical description of the three turbulent components over flat, homogeneous (smooth) terrain. The Solari model does not include the crosswind components. We are fortunate, however, that a significant effort has gone into developing models for each component based on a series of high-resolution measurements taken over uniform terrain in Kansas and Minnesota. The work by Kaimal, et al.[6] and Kaimal [7] produced the first systematic modeling of the turbulence characteristics found there. Since then, other investigators have added to and refined this landmark work. Recent work by Højstrup [8,9] and Olesen, Larsen, and Højstrup [10] (subsequently referred to collectively as RISO) provide one of the latest improvements. We have chosen the RISO models as our *smooth terrain reference*.

The author's approach to develop velocity spectral models has been to use the RISO models as references and then to derive empirical scaling factors for each wind farm locale. The information to accomplish this came from a series of extensive measurements from two 50-m towers located immediately up- and downwind of the wind farm. The tower instrumentation included sensitive cup anemometers and vanes at elevations of 5, 10, 20, and 50 m, and a three-axis sonic anemometer at the nominal hub height of 23 m. Also included were measurements of dry-bulb and dewpoint temperatures, temperature difference, and barometric pressure. We used respective subsets of 812 and 633 30-minute records from the up- and downwind towers for determining the local scaling factors.

It has become the practice to model turbulence spectra in terms of the expression

$$nS(n)/u_*^2 = Af^\gamma/(1+Bf^\alpha)^\beta \qquad (1)$$

where $f = nz/U$ and A, B, α, β, and γ are constants that depend local atmospheric conditions. Figure 1 schematically describes such a model.

The constants of Equation (1) determine the shape and position of the predicted spectrum. Constants A and B control the position of the spectral peak, denoted by f_m, along the reduced frequency axis. The overall spectral shape is determined by the values of α, β, and γ. The values of these constants are developed using Monin-Obukhov (M-O) similarity theory. This theory hypothesizes that the mean flow and turbulence characteristics depend only on four independent variables in a horizontally homogeneous surface layer: the elevation z, friction velocity u_*, kinematic heat flux $H_0/\rho c_p$, and buoyancy g/T_0. Sometimes, it is convenient to include more than one of the

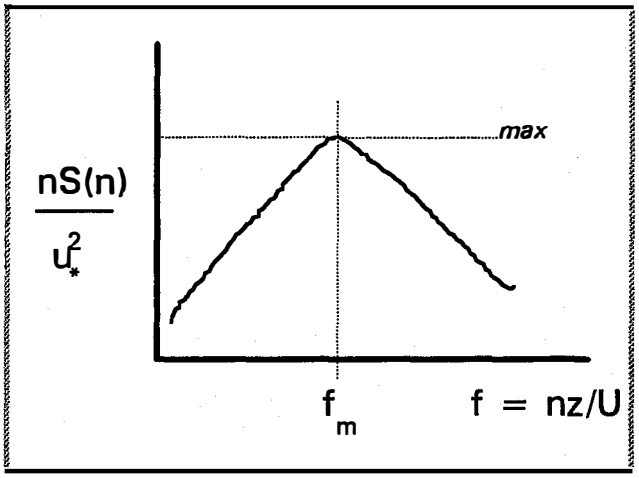

Figure 1. Schematic of spectrum with scaling parameters indicated

scaling parameters in a new one (e.g., z/L is a measure of stability and the reduced frequency is f = nz/U). For unstable flows (z/L < 0), the depth of the mixed layer or the height of the first temperature inversion z_i is also included.

The author established empirical relationships between the observed spectral peaks normalized by u_*^2 and the corresponding reduced frequencies $f_{m,i}$ from the hub-level sonic anemometer at each tower location. It was necessary to use the hub-height or local value of u_* measured directly by the anemometer, $-\left(\overline{u'w'}\right)^{1/2}$, rather than the value calculated from the vertical wind profile, u_{*_o}. We believe this was made necessary by the presence of the massive wind farm, which produces a deviation from the log wind profile model at both locations, as well as a locally distorted upwind flow field and increased shear stress in the downwind (internal) flow caused by decaying wakes from upwind turbines. This deviation was quantified by establishing empirical relationships between the local value derived from the sonic anemometer and the expected value of u_* predicted by the *diabatic* log wind profile, expressed as

$$u_{*_o} = U_{ref}\left[\frac{\kappa}{\ln(z_{ref}/z_o) - \psi_m(z/L)}\right] \qquad (2)$$

Derived from first principles, Equation (2) provides a reasonable estimate of u_* over smooth terrain. The diabatic term ψ_m is zero for neutral flows (z/L = 0), negative for unstable flows (z/L < 0), and positive (z/L > 0) for stable flows. The u_*/u_{*_o} relationships are summarized in Figure 2 for each tower and stability classification. Under neutral conditions, the ratio is 1.0 and 1.4 for the up- and downwind towers, respectively. For stable flows over *uniform terrain* (where M-O similarity applies), a single scaling expression is usually sufficient, or

$$nS_i(n) / u_*^2 = F(f, z/L) \qquad (3)$$

where i = *u*, *v*, and *w*, and u_*, f, and z/L are the scaling parameters. The horizontal wind components (*u*,*v*) in unstable flows do not follow M-O scaling. Kaimal [7] established

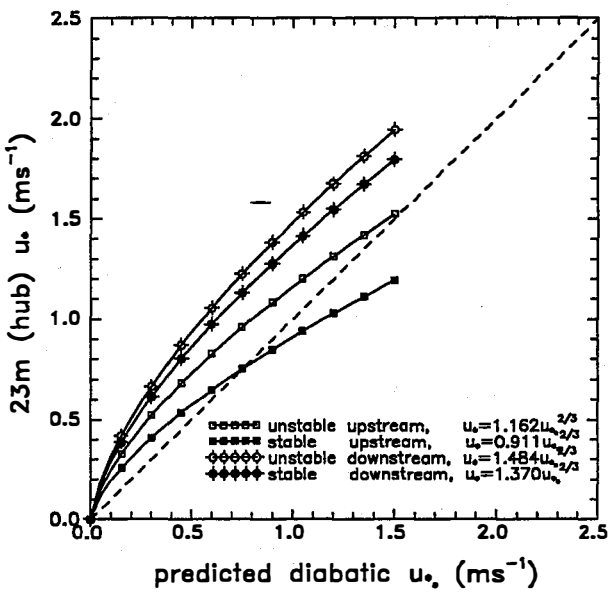

Figure 2. Ratio of observed hub-elevation local u_* to predicted diabatic u_{*_o} for stable and unstable conditions at the upwind and downwind towers

that turbulent spectra in unstable flows could be modeled as the sum of two spectral peaks:

$$S(n) = S_L(n) + S_H(n) \qquad (4)$$

where $S_L(n)$ and $S_H(n)$ are independent low- and high-frequency spectral contributions from the effects of buoyancy and shear, respectively. The pertinent scaling parameters for the *u* and *v* components in unstable flow are u_*, f_1, and z/L. The mixed layer depth z_i, which was not measured directly, has been estimated using the expression

$$z_i \approx .04 U_{hub}/f_c \log_{10}(z_{hub}/z_o) \qquad (5)$$

where $f_c = 1.46\times10^{-4}\sin(33.9°)$. Spectral scaling is accomplished by finding empirical relationships defining the spectral peak of Equation (1) or $[nS(n)/u_*^2]_{max}$ and its corresponding reduced frequency f as functions of the stability parameter z/L. For unstable flows involving the horizontal wind components *u* and *v*, the stability parameter is the ratio of z_i and L and is designated z_i/L (or $z_i/-L$ for ease of analysis and plotting purposes). The reduced frequency is denoted as f_m except when z_i scaling is used, when it is designated f_i.

To identify the observed spectral peaks, we stratified the available 30-minute data sets first by stability and then by mean wind speed. Stability classifications included unstable (Ri < 0), near-neutral (0 ≤ Ri < 0.01), and stable (Ri ≥

0.01). These stability classes were then subdivided into wind speed classes of 2 ms^{-1} in width. The logarithmically smoothed frequency spectra and scaling parameters derived from each 30-minute record for each subclass were then ensemble-averaged. The spectral peaks, $[nS(n)/u_*^2]$, and corresponding reduced frequencies, (f_m, f_i), were determined by eye from of each of the smoothed spectral plots.

It was found necessary to include, depending on the stability (z/L), up to three spectral peaks to describe the observed spectral variance distributions. For example, two peaks were needed to describe the spectra for all three wind components from the upwind tower in *both* stable and unstable flows. The downwind spectra were similar, but a third and highest frequency peak was necessary for the crosswind (v) component in unstable flow conditions. This high-frequency (small wavelength) peak appears to be associated with decaying wakes from upwind turbines. Any accompanying peaks in the streamwise and vertical spectra were found to be indistinguishable apparently as a result of the intense vertical mixing associated with the strong convection rising from the desert floor. Therefore, the model for the unstable v-component is

$$S_v(n) = S_L(n) + S_H(n) + S_{wake}(n) \qquad (6)$$

The two peaks found necessary to describe the spectra from both towers under stable conditions are in contrast to the single peak usually identified with flows over flat terrain. The low-frequency peak for the stable upwind flows is apparently related to the steep and complex terrain surrounding the site. Gravity-driven downslope or drainage winds are probably a major contributor, particularly at night. The high-frequency content is most likely a shear contribution. A case could possibly be made for including a third and higher frequency peak for the stable flows at the downwind tower (i.e., a low-frequency terrain-induced contribution, a midfrequency shear input, and a high-frequency upwind turbine wake component). The author believes, however, that the latter two dominate over the target period of 10 minutes; as a result, he has included only two peaks in the final model.

Empirical relationships describing the variation in the reduced frequency associated with the spectral peaks as a function of stability (z/L) were developed in a two-stage process. First, scaling equations were derived using both linear and nonlinear regression. Then, the relationships predicted by these regression equations were compared with the observed ensemble-averaged spectra for each subclass. An iterative adjustment was then performed over the range of available subclasses to achieve a reasonable consensus for the full observational range, i.e., all stability and wind speed classes. As an example, Figure 3 summarizes the results of this process for the downwind tower in stable flow. The derived scaling relationships for the low- and high-frequency ranges are shown before and after the iterative adjustment. The relationships predicted by the RISO smooth terrain model are only plotted for the low-frequency range because there is no equivalent for high frequencies.

The final relationships relating spectral peaks and reduced frequencies for both towers were used to form *scaling ratios* (Ψ, Φ) with the RISO model as functions of z/L, f_m, and f_i. These ratios allow us to adjust the spectral scaling predicted for smooth terrain to reflect local conditions. For example, the scaling for Højstrup's model [9] for the unstable u-component at the downwind tower is

$$nS_u(n)/u_*^2 = \Psi_L[(0.5\Phi_L f_i)(z_i/L)^{2/3}/(1 + 2.2\Phi_L f_i^{5/3})] + \Psi_H[\{(105 f_{ru})(1 - z/z_i)^2\}/ \{(1 + 33 f_{ru})^{5/3}(1 + 15 z/z_i)^{2/3}\}] \qquad (7)$$

where $f_{ru} = f/(1 + 15\, z/z_i)$ and Ψ_L, Ψ_H, Φ_L, and Φ_H are the spectral peak and positional scaling ratios for local and smooth terrain for the high- and low-frequency ranges.

An example of the results of this scaling process is presented in Figure 4. The predicted spectral distributions of the turbulent u', v', and w' components are plotted for smooth terrain up- and downwind of the San Gorgonio wind farm. Each spectrum is for a mean hub-height wind speed of 12 ms^{-1} and surface roughness of 0.01 m. Three stability conditions are shown that commonly occur during the *day* (unstable), the *transition* from day to night (near-neutral), and the *night* (stable). In general the spectral peaks near the wind farm occur at lower frequencies (longer periods) than they do over smooth terrain. Also, the high levels of turbulent energy observed in the wind farm crosswind component (v') are clearly accounted for.

SPATIAL COHERENCE

The *vertical* coherence is modeled as a decaying exponential in terms of the coherence decrement b, defined as

$$\underset{i}{\mathrm{Coh.}}(z) = \exp[-b(f\Delta z/U)] \qquad (8)$$

where i = u, v, and w, b is the decrement, and Δz is the vertical separation distance. In this paper, we define Coh based on the *coherence-squared* function. A more general definition would include Δr, the separation including increments of Δx and Δy as well as Δz. Measurements including Δx and Δy are rare, and none of which we are aware have been taken in and around a functional wind farm. Coherence measurements from vertical towers are much more commonplace and were calculated from the San Gorgonio data sets.

Davenport [11] initially defined the vertical coherence of the horizontal wind speed as

$$\mathrm{Coh}(z) = \exp(-b_{d10} f\Delta z / U_{10}) \qquad (9)$$

where U_{10} is mean wind speed at the reference anemometer height of 10 m and b_{d10} is the corresponding decrement derived from the *square root of the coherence function*. Veers used Solari's definition of spatial coherence (which is also based on the *square root of the coherence function*) between points within the simulated rotor disk defined as

$$\mathrm{Coh}_{jk} = \exp(-C_{jk} f\Delta r_{jk} / U_{jk}) \qquad (10)$$

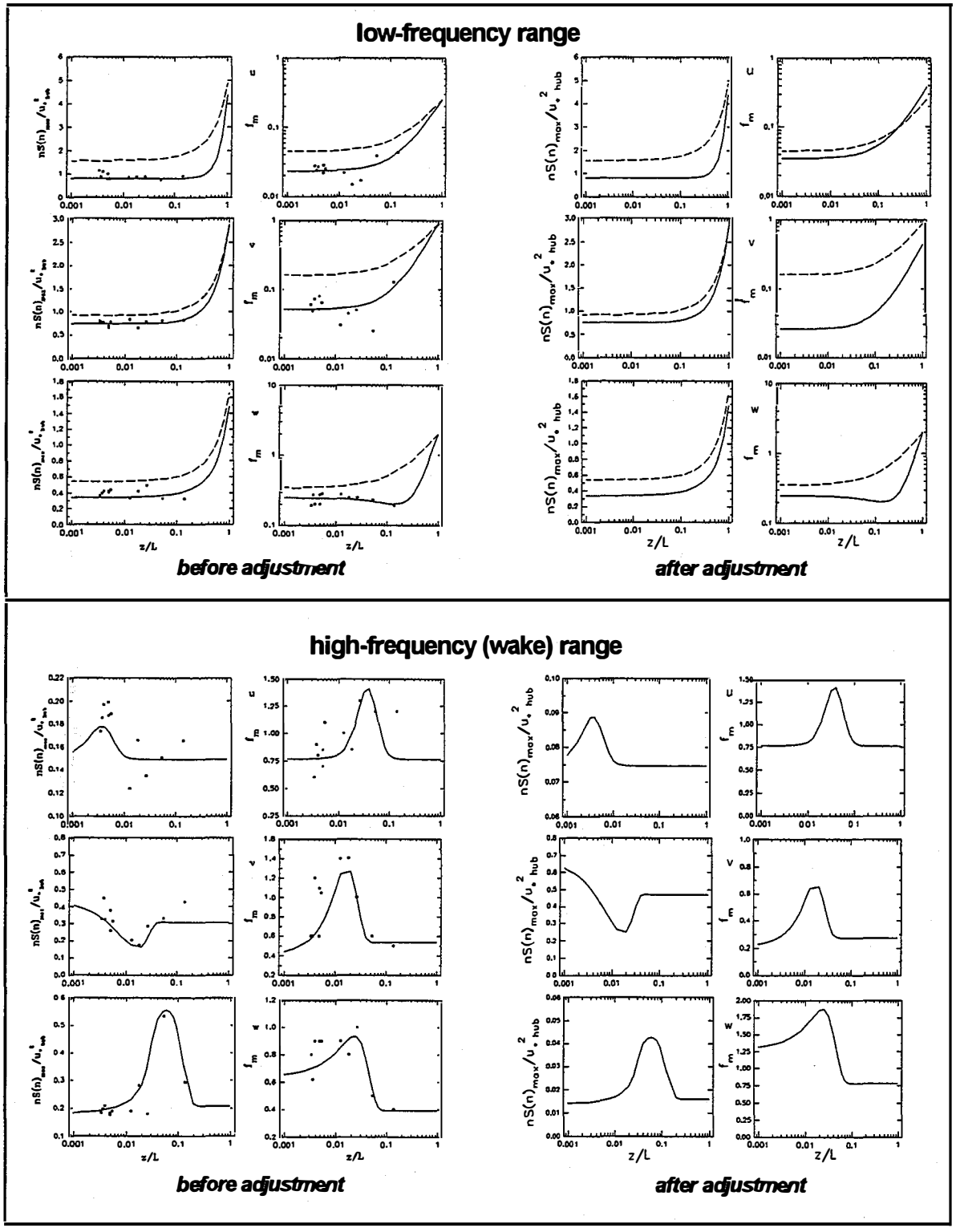

Figure 3. Observed (*solid*) and predicted (*dashed*) equivalent smooth terrain spectral peak scaling for stable flow at the downwind tower before and after iterative adjustments

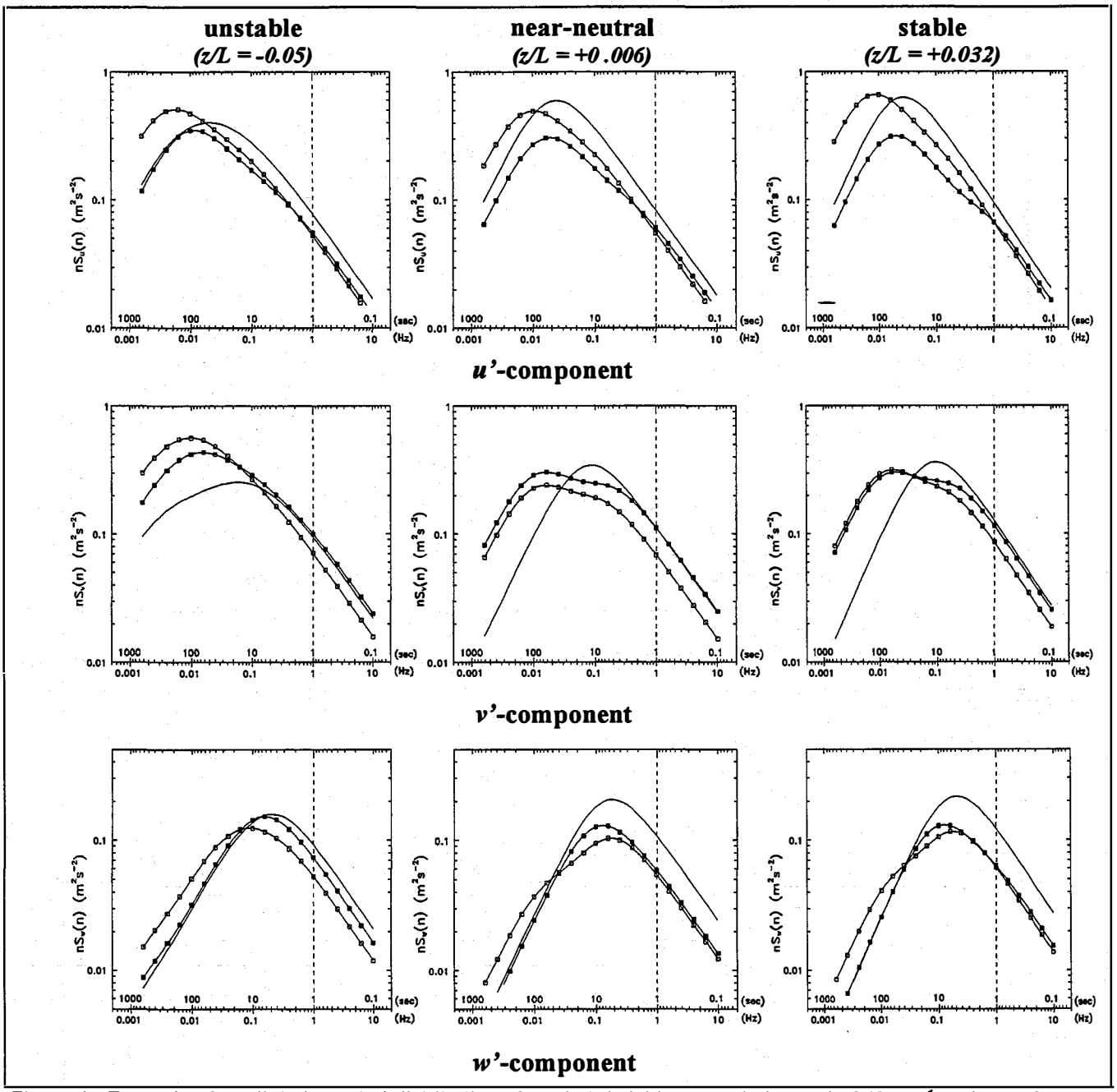

Figure 4. Example of predicted spectral distributions for a hub-height mean wind speed of 12 ms^{-1} and a surface roughness of 0.01 m. Smooth terrain spectra are shown as (——), upwind tower as (□), and the downwind tower as (■)

where $C_{jk} = b(\Delta r_{jk} / z_m)^{0.25}$, $z_m = (z_j + z_k)/2$, $U_{jk} = (U_j + U_k)/2$, and $b = 12 + 5\mathbf{U}[-1,1]$.

The vertical coherence of the streamwise (u) and crosswind (v) components were calculated for each of the 30-minute records available from the two towers in the San Gorgonio wind farm. The *coherence-squared* function was determined for nine of the ten combinations of available vertical separations. Decrements were then calculated for the Davenport and the Solari models with the C_{jk} exponential for the latter set to 0 and 0.25 (Veers refers to the former as the *standard exponential form*).

Figure 5 plots the observed correlation coefficients for each of the decrement models. The "standard" and Solari models have definite advantages over the decrement referenced with the 10-m mean wind speed, particularly at the lower speeds. The

differences between a coherence exponent of 0 and 0.25 are not great, with the former showing a slight improvement over the later at moderate to high wind speeds. The observed vertical coherence decrements based on the Solari model and the coherence-squared definition are shown in Figure 6. The observed

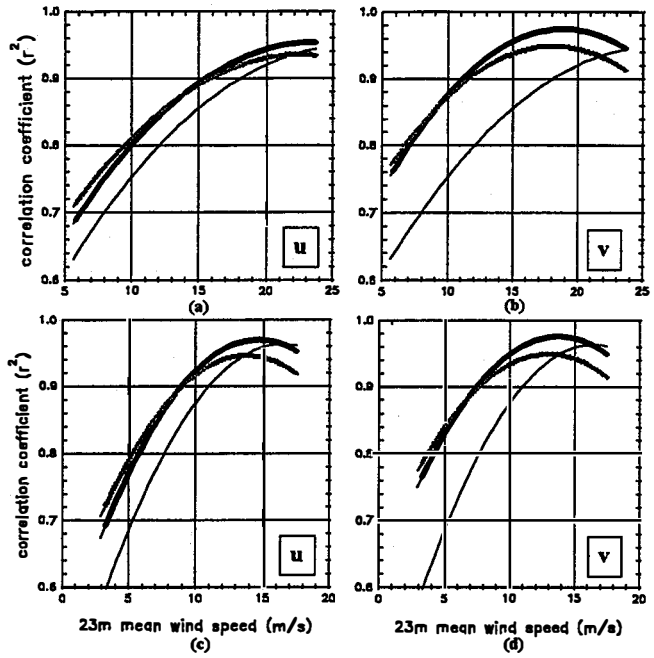

Figure 5. Observed correlation coefficients for coherence models: Davenport 10-m reference (——), "standard" coherence (▬▬), and Solari (▬▬). The vertical coherence correlations for the *u* and *v* components are shown in (*a*) and (*b*) for the upwind tower and (*c*) and (*d*) for the downwind tower

decrements are monotonic with mean wind speed, as indicated by the linear regression line. The darker symbols represent the locally weighted mean values for a given wind speed. The relationships between the mean hub-height wind speed and the coherence decrements for the *u* and *v* components are as follows:

Upwind Tower

$$b_u = 0.923U_{hub} \quad (\pm 2.49)$$
$$b_v = 0.700U_{hub} \quad (\pm 1.93)$$

Downwind Tower

$$b_u = 0.993U_{hub} \quad (\pm 1.78)$$
$$b_v = 0.826U_{hub} \quad (\pm 1.63)$$

It was not possible to calculate a decrement for the vertical component because only a single level measurement was available. The area at the bottom of each graph indicates the expected range of variation according to Solari. The ordinate values would be twice those shown if the square root of the coherence function were used.

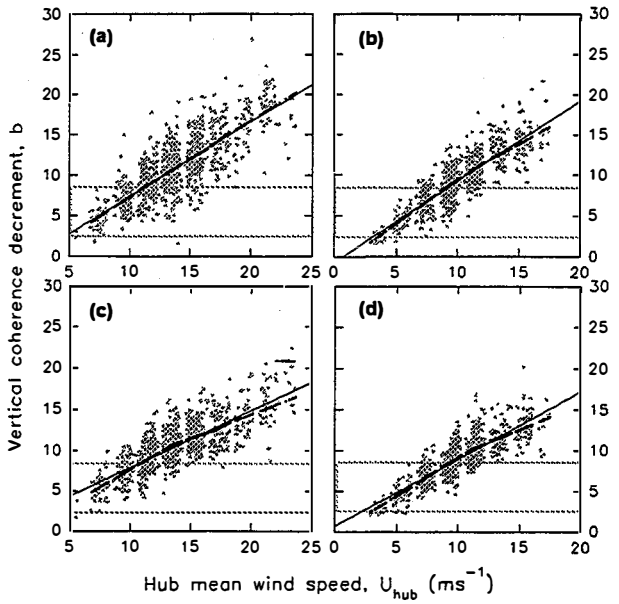

Figure 6. Observed vertical coherence decrements based on the Solari coherence model and the *coherence-squared* function. The *u*-component decrements are shown in (*a*) and (*b*) for the up- and downwind towers. The *v*-component decrements are shown in (*c*) and (*d*). The area at the bottom of each graph represents the uniformly distributed range suggested by Solari

CROSS-AXIS CORRELATION

Our initial analysis of the side-by-side turbine test data [4] has shown what the author believes to be a significant relationship between extreme structural load events and the degree of cross-axis correlation shown by the three wind components measured at hub height. Such correlations are indicative of coherent turbulent structures embedded in the more random general flow. There are several fluid dynamics parameters, which are functions of the flow, that can be used to describe such correlated structures. Two of these are the Reynolds stresses τ_{ij}, derived from the cross-axis covariances $\left(\overline{u'w'}\right)$, $\left(\overline{u'v'}\right)$, and $\left(\overline{v'w'}\right)$ and the normalized cross-axis correlation functions r_{ij}. We have measured both and, at least for now, have chosen to use the r_{ij} in the time domain to introduce cross-axis correlation into the simulated wind components. To this end, we have established empirical relationships between the r_{uw}, r_{uv}, and r_{vw} coefficients and the stability parameter z/L and mean wind speed U_{hub}. After examining the results using the measured r_{ij} coefficients to crossfeed the simulated velocity components, we found that only the *u*-component needed to be crossfed with the *v*- and *w*-components using the expression

$$u(t) = u(t) + \overline{r_{uv}}v(t) + 2\overline{r_{uw}}w(t) \; . \qquad (11)$$

to achieve simulated mean Reynolds stresses ($\tau_{ij} = -\rho\overline{u_i' u_j'}$) equivalent to those observed. We have measured for the upwind tower in unstable flows

$$\overline{r_{uv}} = -1.14(z/-L) + 0.011(U_{hub}/u_*) - 0.292$$

$$\overline{r_{uw}} = -0.142u_* - 0.305$$

and, for stable flows,

$$\overline{r_{uv}} = -0.034(z/L) - 0.136u_*$$

$$\overline{r_{uw}} = 0.038(z/L) - 0.079u_* - 0.325$$

The correlations for the downwind tower in unstable flows are

$$\overline{r_{uv}} = -0.018(z/-L) + 0.016$$

$$\overline{r_{uw}} = -0.021(z/-L) - 0.117u_* + 0.013(U_{hub}/u_*) - 0.373$$

and, for stable flows, they are

$$\overline{r_{uv}} = 0.0298(z/L) + 0.022$$

$$\overline{r_{uw}} = -0.051u_* + 0.006(U_{hub}/u_*) - 0.398$$

Little information is available for the smooth terrain models in this form. Experimentation has suggested the following:

$$\overline{r_{uv}} = 0$$

$$\overline{r_{uw}} = -0.250.$$

CONCLUSIONS

Veer's original model framework has served as an excellent vehicle for simulating the three-dimensional turbulent wind vector within a HAWT rotor disk. An analysis of the turbulent environments up- and downwind of a large wind farm located near very complex terrain have shown the following:

- Peak turbulence levels occur at longer wavelengths or periods than usually occur over smooth terrain
- The crosswind (v) component contains considerably more turbulent energy than is expected over smooth terrain, particularly during unstable flow conditions
- Observed velocity spectra can be modeled as the sum of two spectral peaks
- The unstable downwind crosswind (v) component is the exception requiring three peaks to describe the spectral distributions
- The vertical coherence of the longitudinal (u) and crosswind (v) turbulent components varies monotonically with the mean hub-elevation wind speed

ACKNOWLEDGMENTS

This work has been supported by the U.S. Department of Energy under contract number DE-AC02-83CH10093. The excellent and timely cooperation afforded us by Paul Veers of the Sandia National Laboratories in this endeavor is sincerely appreciated. Appreciation is also extended to Gary Desrochers of NREL for his support of the work through programming and analysis.

REFERENCES

[1] Veers, P.S., March 1988, "Three-Dimensional Wind Simulation," SAND88-0152, Sandia National Laboratories, Albuquerque, NM.

[2] Veers, P.S., September 1984, "Modeling Stochastic Winds on Vertical Axis Wind Turbines," SAND83-1909, Sandia National Laboratories, Albuquerque, NM.

[3] Kelley, N.D., and Wright, A.D., October 1991, "A Comparison of Predicted and Observed Turbulent Wind Fields Present in Natural and Internal Wind Park Environments," NREL/TP-257-4508, National Renewable Energy Laboratory, Golden, CO.

[4] Tangler, J., Smith, B., Jager, D., and Olsen, T., September 1990, "Atmospheric Performance of the Special-Purpose SERI Airfoil Family: Final Results," SERI/TP-257-3939, National Renewable Energy Laboratory, Golden, CO.

[5] Solari, G., July 1987, "Turbulence Modeling for Gust Loading," *ASCE J. Struct. Engineering*, Vol.113(7).

[6] Kaimal, J.C., Wyngaard, J.C., Izumi, Y., and Cote, O.R., 1972, "Spectral Characteristics of Surface Layer Turbulence,". *Quart. J. Royal Meteorological Society*, Vol. #98.

[7] Kaimal, J.C., January 1978, "Horizontal Velocity Spectra in the Unstable Surface Layer," *J. Atmos. Sci.*, Vol. #35.

[8] Højstrup, J., 1981, "A Simple Model for the Adjustment of Velocity Spectra in Unstable Conditions Downwind of an Abrupt Change in Roughness and Heat Flux,". *Boundary-Layer Meteorology*, Vol. #21.

[9] Højstrup, J., October 1982, "Velocity Spectra in the Unstable Planetary Boundary Layer,". *J. Atmos. Sci.*, Vol. #39.

[10] Olesen, H.R., Larsen, S.E., and Højstrup, J., 1984 "Modeling Velocity Spectra in the Lower Part of the Planetary Boundary Layer," *Boundary-Layer Meteorology*, Vol. #29.

[11] Davenport, A.G., 1961, "The Spectrum of Horizontal Gustiness Near the Ground in High Winds,". *Quart. J. Royal Meteorological Society*, Vol. #87.